Rate Allocation for 2-User MAC with MMSE Turbo Equalization

Marcus Grossmann, Thomas Ortlepp, and Tad Matsumoto, *Senior Member, IEEE*

***Abstract*—We consider the problem of rate allocation in frequency-selective 2-user Gaussian multiple access fading channels employing turbo equalization. The turbo equalization framework used in this paper contains a soft cancellation frequency domain minimum mean squared error equalizer and two a posteriori probability channel decoders. Using the relationship between the rate of any code and the area under its corresponding decoder extrinsic information transfer (EXIT) function, we derive an upper bound on the rate region of the 2-user turbo system, given the EXIT characteristic of the equalizer for a particular channel realization. With the rate region upper bound, we then study the problem of maximizing the sum rate of both users, and provide an approximate solution to this optimization problem. Based on the obtained result, a practical code selection algorithm for rate allocation at both transmitters is proposed. In addition, we discuss the extension of the proposed algorithm to an outage-based rate allocation approach. Numerical results of capacity calculations and throughput simulations are presented to demonstrate the performance enhancement achieved by the proposed rate allocation technique over automatic repeat request with fixed coding rate.**

***Index Terms*—Two-user multiple access channel, rate allocation, extrinsic information transfer chart analysis, minimum mean squared error equalization.**

I. Introduction

RECENTLY, iterative (turbo) techniques have been recognized as practical solutions to multi-user detection/equalization problems in coded communication systems. In [1], utilization of the optimal a posteriori probability (APP) equalizer (EQ) in combination with the APP-based decoder (DEC) is considered for turbo equalization in frequency-selective fading channels. The turbo EQ of [1] achieves excellent performance, however, its complexity is prohibitively high in channels having a medium-to-large number of multipath components. In [2], the APP detector (DET) is replaced by a less complex DET that performs soft canceling and minimum mean squared error (SC MMSE) filtering. This SC MMSE filtering approach, originally proposed for detection of random coded code-division multiple-access (CDMA) signals, is applied to channel equalization in [3], and to multiple-input multiple-output (MIMO) channel equalization in [4]. In [5], a turbo equalization technique for single carrier block-transmission over multiple-access channels (MACs) in the presence of frequency-selective fading is proposed that performs the SC MMSE filtering in frequency domain, further reducing the computational complexity.

The convergence of turbo systems can be analyzed by extrinsic information transfer (EXIT) charts [6]. The EXIT chart may be used to predict the convergence threshold and to visualize the mutual information (MI) exchange between the soft-input soft-output components, representing the convergence property of turbo systems. Ashikhmin *et al.* [7] showed that for any code with rate R, the area under its corresponding DEC EXIT function is $1 - R$. This property has been proved so far only for the case when the DEC's *a-priori* information is assumed to be from an erasure channel. However, it also appears to work well for Gaussian distributed *a-priori* log-likelihoods (LLRs) [7]. Based on the area property of the EXIT chart, it has been shown in [8], [9] that the problem of rate allocation in the *single-user* case, in general, reduces to a simple curve-fitting problem of the two-dimensional (2D) EXIT curves of the DET and DEC. In [8], ten Brink *et al.* used this technique to determine the optimal degree distribution of low density parity check (LDPC) codes for single-user MIMO bit interleaved coded modulation (BICM) employing iterative detection and decoding. Based on a similar idea, the authors of [9] investigate the design of repeat-accumulate codes with iterative detection.

The EXIT chart can also be used for rate allocation in MAC scenarios. In [10], the EXIT chart analysis is used to optimize LDPC codes for the *equal-rate* 2-user Gaussian MAC without fading employing iterative decoding. It is shown that for allocating the same rate to both users very simple LDPC code optimization approaches can be derived, similarly to the single-user case. Similar results with LDPC codes are obtained in [11], where the authors showed that by properly choosing the multi-user code and applying iterative decoding, any point on the boundary of the capacity region can be closely approached without requiring time-sharing [12] or rate-splitting [13].

The EXIT chart analysis is used in [14] to optimize LDPC codes for the *equal-rate* flat-fading MIMO MAC employing iterative detection and decoding. The problem of rate allocation is studied from a large-system perspective, i.e., the number of users and antennas are taken to infinity, while their ratio remains fixed. For such a system, it is shown that results from the asymptotic analysis of CDMA with random spreading remains valid, which allows the behavior

Manuscript received July 8, 2008; revised March 31, 2009 and October 7, 2009; accepted October 15, 2009. The associate editor coordinating the review of this paper and approving it for publication was D. Gesbert.

M. Grossmann and T. Ortlepp are with Institute for Information Technology, Ilmenau University of Technology, Germany (e-mail: {marcus.grossmann, thomas.ortlepp}@tu-ilmenau.de).

T. Matsumoto is with Japan Advanced Institute of Science and Technology, Japan, and Center for Wireless Communication at University of Oulu, Finland (e-mail: matumoto@jaist.ac.jp).

This work was supported in part by the German Research Foundation (DFG) under grant SPP1163 and in part by the Japanese government funding program, Grant-in-Aid for Scientific Research (B), No. 20360168.

Digital Object Identifier 10.1109/TWC.2010.03.080894

of the iterative receiver to be described by a single 2D EXIT chart. Thus, rate allocation is performed by 2D EXIT curve matching, as in the single-user case. The results reveal that with the system proposed in [14] near capacity performance can be asymptotically achieved. Asymptotic techniques for rate allocation have also been applied in [15] to design repetition codes in the context of *equal-rate* CDMA systems with iterative detection and decoding.

In this paper, we consider the problem of rate allocation for the 2-user frequency-selective fading MAC employing soft cancellation frequency domain MMSE (SC FD-MMSE) equalization. In contrast to previous work [10], [14], [15], we do not restrict the rates of both users to be equal. For such a turbo system, the EQ EXIT characteristic is given by two 3D surfaces, and thus, rate allocation is no longer a simple 2D matching of the EXIT chart.

Based on the area property of EXIT functions, we derive an upper bound on the rate region of the 2-user turbo system, given the EQ EXIT functions for a particular channel realization and receiver noise variance. The rate region upper bound is then used to study the problem of maximizing the sum rate of both users. Specifically, we show that the sum rate maximization can be formulated as a variational problem. We provide an efficient solution to this optimization problem by using an approximation on the EQ EXIT functions. As a result, the optimal DEC EXIT curves of both users with respect to the maximum sum rate of the turbo system, are obtained.

For practical reasons, we restrict each transmitter to have only a finite number of codes with fixed rates. For this scenario assumption, we propose a simple *code selection* algorithm for the rate allocation that maximizes the coding rate of each user, given the optimal DEC EXIT curve, while satisfying the constraints for successful decoding. Moreover, we discuss as an extension of the proposed algorithm an outage-based rate allocation approach, and determine the achievable coding rates of both users using a specific *outage* constraint.

The remainder of this paper is organized as follows. The notation is introduced in Section II. In Section III, the system description and the channel model are presented. In Section IV-A, we define the EXIT functions for the EQ and both DECs, and derive an upper bound on the rate region of the 2-user turbo system. We then consider the optimization of the sum rate of both users in Section IV-B and propose a simple rate allocation algorithm in Section IV-C. In Section IV-D, we extend the proposed algorithm to an outage-based rate allocation approach. In Section V, we present some numerical results to verify the performance of the proposed approaches. We summarize our results in Section VI.

II. Notation

The transpose and conjugate transpose operators are denoted by $(\cdot)^T$ and $(\cdot)^H$, respectively. The $\text{circ}_Q\{\mathbf{a}\}$ operator generates an $Q \times Q$ circulant matrix having the elements of vector $\mathbf{a}$ on its first column. The symbol $\otimes$ indicates the Kronecker product. The notation $\mathbf{a} \geq \mathbf{b}$ for length-N vectors $\mathbf{a}$ and $\mathbf{b}$ means $a_n \geq b_n$ for $n = 1, .., N$. We use the symbol $\equiv$ to indicate that the expression on the left hand side is defined by the expression on the right hand side. We use $\mathbb{E}^n$ to represent a closed set $\mathbb{E}^n \equiv \{\mathbf{x} \in [0,1]^n\}$, and $\partial\mathbb{E}^2$ is used for the boundary of $\mathbb{E}^2$. We denote the four corner points of the region $\mathbb{E}^2$ by $a_0 \equiv (0,0)$, $a_1 \equiv (0,1)$, $a_2 \equiv (1,1)$ and $a_3 \equiv (1,0)$. Finally, $\mathcal{F}^1[a,b]$ denotes the space of monotonically increasing, continuous and piecewise differentiable functions on the interval $[a,b]$.

III. System Model

Consider a single carrier cyclic prefix (CP) assisted 2-user uplink system, where a base station having M receive antennas receives signals from two active users, each equipped with K transmit antennas. For the ease of analysis, we assume in the following $M = 2$ and $K = 1$. However, the extension to more generic cases ($M > 2$, $K > 1$) is straightforward. The transmission scheme of each user is based on BICM, where the information bit sequence is independently encoded by a rate-$r_{c,k}$ (with $k = 1, 2$ being the user index) binary encoder, randomly bit-interleaved, binary phase-shift keying (BPSK) modulated, and grouped into N ($n = 1, .., N$) blocks $\mathbf{b}_k(n) \equiv \left[b_{0,k}(n), ..., b_{q,k}(n), ..., b_{Q-1,k}(n)\right]^T$ of length Q that are transmitted over the frequency-selective fading MAC. The binary encoder can be a single convolutional code (SCC) or a serially concatenated convolutional code (SCCC) [22]. Note that throughout the paper, we use index k to denote user k.

The frequency-selective fading MAC is assumed to be constant during the transmission of one frame (comprised of N blocks), but varying randomly and independently frame-by-frame. We restrict ourselves to Rayleigh block-fading channels, where each of the $2KM$ links is comprised of L independent and identically distributed (i.i.d.) complex circularly-symmetric Gaussian path components $\mathbf{h}_{k,m} \equiv \left[h_{k,m}(0), ..., h_{k,m}(L-1)\right]^T$ for $m = 1, ..., M$. We always assume that all channel gains are perfectly known at the receiver.

Employing a CP of length $P = L - 1$ to each transmit block, the received signals can be expressed as

$$\mathbf{r}(n) = \sum_{k=1}^{2} \mathbf{H}_k \mathbf{b}_k(n) + \mathbf{v}(n), n = 1, .., N, \tag{1}$$

where $\mathbf{H}_k = \left[\mathbf{H}_{k,1}^T \quad \mathbf{H}_{k,2}^T\right]^T$ with $\mathbf{H}_{k,m} = \text{circ}_Q\{\mathbf{h}_{k,m}\}$ being the block-circulant channel matrix associated to the k-th user, and $\mathbf{v}(n) \sim \mathcal{CN}(\mathbf{0}, \sigma^2\mathbf{I})$ is the additive white Gaussian noise (AWGN). Note that each $\mathbf{H}_k$ may be decomposed into a diagonal-block matrix $\mathbf{\Xi}_k$ by the Fourier matrix,

$$\mathbf{H}_k = (\mathbf{I}_2 \otimes \mathbf{F}^H)\mathbf{\Xi}_k\mathbf{F}, \tag{2}$$

where $\mathbf{F}$ denotes the Fourier matrix of size Q, whose (l,j)-th element is given by $(1/\sqrt{Q})\exp(-i2\pi lj/Q)$, $i = \sqrt{-1}$, for $0 \leq l, j \leq Q-1$.

At the receiver side, iterative processing for joint equalization and decoding is performed. The receiver consists of an SC FD-MMSE EQ and two single-user DECs that perform APP decoding. It should be noted here that the major outcomes of this paper are also applicable to other types of equalization techniques.

Within the iterative processing, *extrinsic* LLRs of the coded bits are exchanged between the EQ and two DECs, each

separated by the interleaver and deinterleaver in their iteration loop, following the turbo principle [2]. Inputs to the EQ are the received signals $\mathbf{r}(n)$ and the *a priori* LLR sequences

$$\boldsymbol{\zeta}_k(n) \equiv \big[\zeta_{0,k}(n), ..., \zeta_{q,k}(n), ..., \zeta_{Q-1,k}(n)\big]^T \text{ for all } n, k, \tag{3}$$

where

$$\zeta_{q,k}(n) \equiv \log\left(\frac{\text{Prob}\big(b_{q,k}(n)=+1\big)}{\text{Prob}\big(b_{q,k}(n)=-1\big)}\right). \tag{4}$$

The EQ computes the *extrinsic* LLR for each transmitted bit $b_{q,k}(n)$,

$$\lambda_{q,k}(n) \equiv \log\left(\frac{\text{Prob}\big(z_{q,k}(n)|b_{q,k}(n)=+1\big)}{\text{Prob}\big(z_{q,k}(n)|b_{q,k}(n)=-1\big)}\right) \tag{5}$$

where $z_{q,k}(n)$ is the SC FD-MMSE filter output as defined in equation (18) in [5]. Similarly to (3), we arrange the $\lambda_{q,k}(n)$'s into vectors $\boldsymbol{\lambda}_k(n) \equiv \big[\lambda_{0,k}(n), ..., \zeta_{Q-1,k}(n)\big]^T$ for all n, k. Note that during the first iteration of turbo equalization, $\zeta_{q,k}(n)$ is zero for all n, k, q, and later on $\zeta_{q,k}(n)$ is provided via the interleaver in the form of *extrinsic* LLRs of the k-th DEC.

The receiver also selects the code to be used for each user from an available code set according to the criterion derived in Section IV-C, where both users are notified of the codes selected through separated feedback links. We assume zero-delay and error-free feedback links.

IV. Rate Allocation

A. Definition of EXIT Functions and Area Property

Let the MI between the transmitted bits $b_{q,k}(n)$ and the corresponding LLRs $\lambda_{q,k}(n)$ be denoted as [5]

$$I_{e,k} \equiv \lim_{N\to\infty} \frac{1}{NQ} \mathrm{I}\big(\mathbf{b}_k(1), ..., \mathbf{b}_k(N); \boldsymbol{\lambda}_k(1), ..., \boldsymbol{\lambda}_k(N)\big),$$

and let the MI between $b_{q,k}(n)$ and $\zeta_{q,k}(n)$ be denoted as

$$I_{d,k} \equiv \lim_{N\to\infty} \frac{1}{NQ} \mathrm{I}\big(\mathbf{b}_k(1), ..., \mathbf{b}_k(N); \boldsymbol{\zeta}_k(1), ..., \boldsymbol{\zeta}_k(N)\big).$$

In the 2-user case the convergence characteristic of the EQ is defined by two EXIT functions,

$$\mathbf{f}_e : \mathbf{I}_d \to \mathbf{f}_e \equiv \big(f_{e,1}(\mathbf{I}_d), f_{e,2}(\mathbf{I}_d)\big) \in \mathbb{E}^2,$$

which depend on the MI $\mathbf{I}_d \equiv (I_{d,1}, I_{d,2}) \in \mathbb{E}^2$ of both DECs. In [5] it is shown that these two EXIT functions can be efficiently computed by modeling the LLRs $\zeta_{q,k}(q) \sim \mathcal{N}\big((\sigma_k^2/2) b_{q,k}(n), \sigma_k^2\big)$ as independent Gaussian random variables, where $\sigma_k = J^{-1}(I_{d,k})$ with J^{-1} being the inverse of J defined as [6]

$$J(\sigma) = 1 - \frac{1}{\sqrt{2\pi}\sigma} \int_{-\infty}^{+\infty} e^{-\frac{(x-\sigma^2/2)^2}{2\sigma^2}} \log_2(1+e^{-x}) \mathrm{d}x. \tag{6}$$

As stated in [3], the filter output $z_{q,k}(n)$ of the EQ can be closely approximated by an equivalent AWGN channel having $b_{q,k}(n)$ as its input,

$$z_{q,k}(n) = \mu_k b_{q,k}(n) + \eta_{q,k}(n), \tag{7}$$

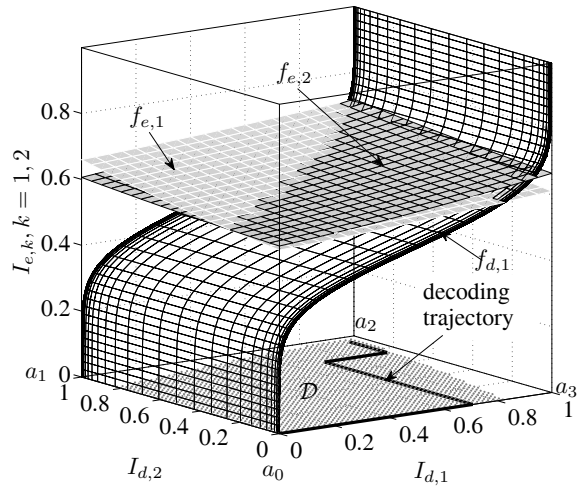

Fig. 1. EQ EXIT functions $f_{e,1}$ and $f_{e,2}$ for a single random channel realization and DEC EXIT function $f_{d,1}$ for a constraint length 5 rate-1/2 SCC. A possible decoding trajectory visualizing the MI exchange over the iterations is plotted as projection onto the plane region $\mathcal{U}$. $Q = 128$, $L = 10$ and $E_s/N_0 = 0$ dB.

where μ_k is the equivalent channel gain, which is conditioned on the FD channel response ($\boldsymbol{\Xi}_1$, $\boldsymbol{\Xi}_2$) and the receiver noise variance σ^2, and $\eta_{q,k}(q) \sim \mathcal{N}(0, \mu_k(1-\mu_k)/2)$. The signal-to-noise ratio (SNR) in (7) is given by $\text{SNR}_k = 2\mu_k/(1-\mu_k)$. Based on (5), the value of $I_{e,k}$ is given by the average MI of the equivalent memoryless binary-input Gaussian channel, as [6]

$$I_{e,k} = f_{e,k}(\mathbf{I}_d) = J\Big(2\sqrt{\text{SNR}_k}\Big). \tag{8}$$

Similarly, the convergence characteristics of both DECs are defined by the two EXIT functions[1] $f_{d,k} : I_{d,k} \to f_{d,k}(I_{d,k}) \in \mathbb{E}$. In addition, these two functions have the extreme values $f_{d,k}(0) = 0$ and $f_{d,k}(1) = 1$ for $k = 1, 2$. We obtain the $f_{d,k}$'s by a Monte Carlo method [6]. In the following, we assume that $\mathbf{f}_e$, $f_{d,1}$ and $f_{d,2}$ are monotonically increasing, continuous and differentiable.

An example of the two EQ EXIT functions $\mathbf{f}_e$ and the DEC EXIT function $f_{d,1}$ is shown in Fig. 1. Also shown is a possible decoding trajectory of the MI exchange, which is plotted as a projection onto the plane region $\mathcal{U} \equiv \{\mathbf{I}_d : \mathbf{I}_d \in \mathbb{E}^2\}$. Note that the DEC EXIT function $f_{d,2}$ (not shown) is drawn in the $I_{d,2}$-coordinate. For the computation of the trajectory, the codes of both users were in this case assumed to be identical, and hence the shapes of their EXIT functions are exactly the same.

Let $\mathcal{D}$ be a region defined by

$$\mathcal{D} \equiv \big\{\mathbf{I}_d : f_{e,k}(\mathbf{I}_d) \geq f_{d,k}(I_{d,k}), k = 1, 2\big\}. \tag{9}$$

The region in (9) is shown in Fig. 1, and is referred to as the *feasible region* of $\mathbf{f}_e$ and $f_{d,k}$, $k = 1, 2$. Note that $a_0 \in \mathcal{D}$, since $f_{e,k}(a_0) \geq f_{d,k}(0) = 0$ for $k = 1, 2$.

Let $\{\mathbf{v}^{(p)}\}$, $\mathbf{v}^{(p)} \in \mathcal{D}$, $\mathbf{v}^{(0)} = a_0$, $p = 0, ..., T$ be a sequence of $\mathbf{I}_d$-tuples that models the decoding trajectory (projected onto the plane region $\mathcal{U}$) according to a specific activation

[1]Note that $f_{d,k}$, denoted in this paper as the DEC EXIT function, corresponds to the inverse DEC EXIT characteristic defined in [6].

ordering of the EQ and the two DECs over T iterations. The monotonicity of all EXIT functions together with the definition in (9) imply that $\mathbf{v}^{(p+1)} \geq \mathbf{v}^{(p)}$ for all p, and thus, the sequence $\{\mathbf{v}^{(p)}\}$ converges monotonically to a limit point $\mathbf{I}_d^* = \lim_{p\to\infty} \mathbf{v}^{(p)}$. As shown in Theorem 1 of [16], this limit point is unique and independent of the actual activation ordering. Convergence of turbo equalization is achieved, when the decoding trajectory attains the maximum point $\mathbf{I}_d^* = a_2$. This is possible for T being sufficiently large, if the following two constraints hold:

$$\mathcal{D} \text{ is pathwise connected}^2 \text{ and } a_2 \in \mathcal{D}. \tag{10}$$

Let $A_{\mathcal{D}} \equiv \iint_{\mathcal{D}} \mathrm{d}\mathbf{I}_d$ be the area of $\mathcal{D}$. Assume now that each DEC EXIT function $f_{d,k}$ is matched to the corresponding EQ EXIT function $f_{e,k}$ so that only an infinitesimally small open tube between the four surfaces remains, where the trajectory can go from $\mathbf{v}^{(0)} = a_0$ to $\mathbf{I}_d^* = a_2$. Note that such DEC EXIT functions imply 1) an ideally designed code for each user of infinite block length to achieve a nearly zero BER and 2) an infinite number of iterations between the EQ and the two DECs[3]. Under this assumption, the size of the area $A_{\mathcal{D}}$ is close to zero and the region $\mathcal{D}$ can be characterized by a curve $\mathcal{S}$, which is referred to as convergence curve in what follows. The convergence curve $\mathcal{S}$ is parameterized by a vector-function

$$\mathbf{u}(t) \equiv \big(u_1(t), u_2(t)\big) : \mathbb{E} \to \mathcal{S}, u_k \in \mathcal{F}^1[0,1], k = 1, 2, \tag{11}$$

where each $u_k(t)$, $t \in \mathbb{E}$ is monotonically increasing in the parameter t and has the prescribed boundary values $u_k(0) = 0$ and $u_k(1) = 1$.

Let $\mathbf{w}_k(\mathbf{u})$ be a three-dimensional space curve, obtained by projection of $\mathbf{u}$ on $f_{e,k}$,

$$\mathbf{w}_k(\mathbf{u}) \equiv \big(u_1(t), u_2(t), f_{e,k}(\mathbf{u}(t))\big) \in \mathbb{E}^3, \tag{12}$$

and let $f_k^{(\mathbf{u})} : I_{d,k} \to f_k^{(\mathbf{u})}(I_{d,k}) \in \mathbb{E}$ be a function obtained by projection of $\mathbf{w}_k$ onto the $I_{d,k}$-$I_{e,k}$-plane. The convergence curve $\mathbf{u} \subseteq \mathcal{D}$ satisfies the constraints in (10), which implies that

$$f_{d,k}(I_{d,k}) < f_k^{(\mathbf{u})}(I_{d,k}), \forall I_{d,k} \in [0,1), \text{ for } k = 1, 2. \tag{13}$$

From (13), we easily obtain the following bound:

$$A_k < A_k^{(\mathbf{u})}, \tag{14}$$

where A_k and $A_k^{(\mathbf{u})}$ denote the areas under $f_{d,k}(I_{d,k})$ and $f_k^{(\mathbf{u})}(I_{d,k})$, respectively,

$$A_k \equiv \int_0^1 f_{d,k}(I_{d,k})\mathrm{d}I_{d,k}, \tag{15}$$

$$A_k^{(\mathbf{u})} \equiv \int_0^1 f_k^{(\mathbf{u})}(I_{d,k})\mathrm{d}I_{d,k}. \tag{16}$$

[2]A set $\mathcal{A}$ is said to be pathwise-connected if for every $p, q \in \mathcal{A}$ there are two real numbers a, b with $a \leq b$ and a continuous mapping f such that $f(a) = p$, $f(b) = q$, and $f([a,b]) \subseteq \mathcal{A}$ [18].

[3]Note that this does not lead to a conclusion that the whole transmission chain can achieve capacity, since the use of sub-optimal (SC FD-MMSE) equalization already incurs a loss in rate [7].

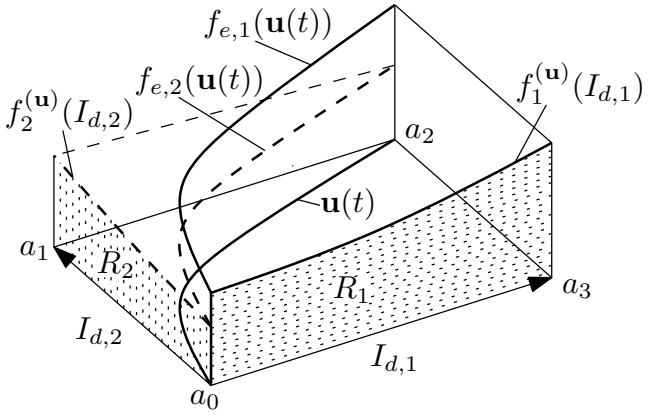

Fig. 2. Example of the parametric convergence curve $\mathbf{u}(t)$ with the two corresponding EXIT space curves and the two areas defining the achievable rates.

In [7], it is shown that the area under the EXIT function $f_{d,k}$ of an APP-based DEC for a rate-R_k code satisfies the property $R_k = A_k$. Combining this result with (14) yields an upper bound for the rate R_k of user k with respect to the convergence curve $\mathbf{u}$,

$$R_k < A_k^{(\mathbf{u})}. \tag{17}$$

Equivalently, the area $A_k^{(\mathbf{u})}$ in (16) can be expressed as line integral of $f_{e,k}$ along $\mathcal{S}$ in $I_{d,k}$-direction, $A_k^{(\mathbf{u})} = \int_{\mathcal{S}} f_{e,k}(\mathbf{I}_d)\mathrm{d}I_{d,k}$. Therefore, we can also express (17) as

$$R_k < \int_{\mathcal{S}} f_{e,k}(\mathbf{I}_d)\mathrm{d}I_{d,k} \tag{18a}$$

$$= \int_0^1 f_{e,k}\big(\mathbf{u}(t)\big)u_k'(t)\mathrm{d}t, \tag{18b}$$

where $u_k'(t)$ denotes the first derivative of $u_k(t)$. The equality in (18b) follows directly from the curve parameterization in (11). An example of the convergence curve with the two corresponding EQ EXIT space curves and related areas defining the achievable rates of both users is shown in Fig. 2.

Let $\mathcal{P}$ be the set of admissible parametric curves in the plane region $\mathcal{U}$,

$$\mathcal{P} \equiv \big\{\mathbf{p} : p_k \in \mathcal{F}^1[0,1], p_k'(t) \geq 0, \forall t, k = 1, 2, \mathbf{p}(0) = a_0, \mathbf{p}(1) = a_2\big\}. \tag{19}$$

From the inequality in (18) and with the definition in (19), we finally obtain an upper bound for the rate region of both users as

$$\mathcal{R} \equiv \bigcup_{\mathbf{p}\in\mathcal{P}} \Big\{(R_1, R_2) : R_k < \int_{\mathbf{p}} f_{e,l}(\mathbf{I}_d)\mathrm{d}I_{d,k}, k = 1, 2\Big\}. \tag{20}$$

Fig. 3 illustrates an example of the rate region in (20), where $f_{e,1}$ and $f_{e,2}$ have been computed using (8) for a random channel realization. The rates at the corner point V_1 can be achieved by successive equalization and decoding techniques, where the signal from user 1 is detected first through iterations only between the EQ and user 1's DEC, such that only the MI $I_{d,1}$ increases with the iterations, while the MI $I_{d,2}$ stays zero. After decoding user 1's signal, the signal from user 2 is iteratively detected, while $I_{d,1} = 1$. Thus, for achieving the

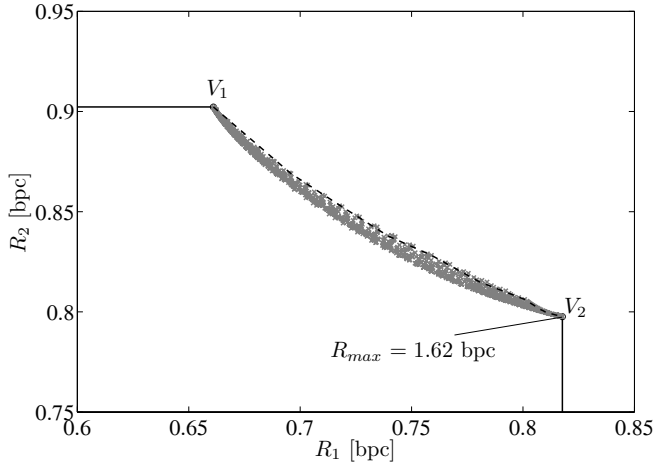

Fig. 3. Rate region of 2-user MAC with SC FD-MMSE turbo equalization for a random channel realization at $E_s/N_0 = 5$ dB, numerically computed by generating a large number of different admissible convergence curves (a gray dot corresponds to one curve). $Q = 32$, $L = 10$.

corner point V_1, the convergence curve $\mathcal{S}$ must be given by a path on the boundary $\partial\mathcal{U}$, which connects the points a_0, a_3 and a_2, $\mathcal{S} = \mathcal{L}(a_0, a_3, a_2)$, where $\mathcal{L}(q_0, q_1, ..., q_v)$ is defined as the union of v straight line segments, connecting the points $q_i \in \mathbb{E}^2$, $i = 0, ..., v$:

$$\mathcal{L}(q_0, q_1, ..., q_v) \equiv \bigcup_{i=0}^{v-1} \big\{q_i + \lambda(q_{i+1} - q_i) : \lambda \in [0, 1]\big\}. \tag{21}$$

The rate tuple at V_2 can similarly be achieved by first iteratively detecting the signal from user 2, followed by user 1's signal detection. In this case the convergence curve must be given by $\mathcal{S} = \mathcal{L}(a_0, a_1, a_2)$. Note that the rate region in (20) is non-convex, in general, where the dominant face of this region strongly depends on the particular realization of the EQ EXIT functions $\mathbf{f}_e$.

B. Maximization of Sum Rate

To identify the rates of both users and the corresponding convergence curve that maximize the sum rate, we are interested to solve the following variational optimization problem:

$$R_{max} \equiv \max_{\mathbf{p}\in\mathcal{P}} \sum_{k=1}^{2} \int_{\mathbf{p}} f_{e,k}(\mathbf{I}_d)\mathrm{d}I_{d,k}. \tag{22}$$

Using (18), the functional in (22) can also be expressed as

$$R[\mathbf{p}(t)] \equiv \int_0^1 Y\big(\mathbf{p}(t)\big)\ \mathrm{d}t, \tag{23}$$

where

$$Y(\mathbf{p}) = \sum_{k=1}^{2} f_{e,k}\big(\mathbf{p}(t)\big)p'_k(t). \tag{24}$$

A first-order necessary condition of optimality to the variational problem is given by the Euler-Lagrange differential equations [17]:

$$\frac{\partial Y(\mathbf{p})}{\partial p_k} - \frac{\mathrm{d}}{\mathrm{d}t}\frac{\partial Y(\mathbf{p})}{\partial p'_k} \stackrel{!}{=} 0, k = 1, 2. \tag{25}$$

Using (24), one can easily check, that the differential equations in (25) reduce to one *algebraic* equation,

$$\frac{\partial f_{e,2}(\mathbf{p})}{\partial p_1} - \frac{\partial f_{e,1}(\mathbf{p})}{\partial p_2} \stackrel{!}{=} 0. \tag{26}$$

The solutions of (26), if they exist, are the candidates satisfying the optimality requirement. However, a direct computation of (26) is not possible, since $f_{e,1}$ and $f_{e,2}$ are not given in closed form. Moreover, the candidate curves of (26) are *stationary paths*, which generally do not satisfy the monotonicity and boundary conditions of (19). Thus, the extremal cannot be obtained directly from (26).

An approximate solution to problem (22) may be derived when each EQ EXIT function $f_{e,k}$ is approximated by a 2D quadratic form[4]

$$f_{e,k}(\mathbf{I}_d) \approx \alpha_{k,0} + \alpha_{k,1}I_{d,1} + \alpha_{k,2}I_{d,2} + \alpha_{k,3}I_{d,1}I_{d,2} + \alpha_{k,4}I_{d,1}^2 + \alpha_{k,5}I_{d,2}^2 \tag{27}$$

with the coefficients $\alpha_{k,i}$ obtained from a standard regression method [18]. Under this assumption, the Euler-Lagrange equations in (25) reduce to one *linear algebraic* equation,

$$T(\mathbf{I}_d) \equiv \frac{\partial f_{e,2}(\mathbf{I}_d)}{\partial I_{d,1}} - \frac{\partial f_{e,1}(\mathbf{I}_d)}{\partial I_{d,2}} \stackrel{!}{=} 0, \tag{28}$$

which leads to three possible outcomes: (i) no solution, (ii) infinite number of solutions, or (iii) a unique solution.

(i) If (28) has no solution, the partial derivatives $\partial f_{e,2}(\mathbf{I}_d)/\partial I_{d,1}$ and $\partial f_{e,1}(\mathbf{I}_d)/\partial I_{d,2}$ are non-equal constants in $\mathbb{R}$. In Appendix A it is shown that in such a case either the boundary curve $\mathcal{L}(a_0, a_3, a_2)$ or $\mathcal{L}(a_0, a_1, a_2)$ solves problem (22). Thus, the sum rate is maximized at the rate region corner point of either V_1 or V_2.

(ii) If (28) has an infinite number of solutions, i.e., curl $\mathbf{f}_e = 0$ for all $\mathbf{I}_d \in \mathbb{E}^2$, the functional in (23) is path-independent [18]. Thus, $R[\mathbf{p}]$ is identical for all $\mathbf{p} \in \mathcal{P}$ and the two corner points V_1 and V_2 are connected by a straight line segment having a decay of -1.

(iii) If (28) has a unique solution, the solution curve $\mathcal{E} \equiv \big\{\mathbf{I}_d : T(\mathbf{I}_d) = 0\big\}$ can be parameterized by a continuous vector-function $\mathbf{g} : \mathbb{E} \to \mathcal{E}$, where the first derivative of $\mathbf{g}$ satisfies $g'_k(t) \geq 0$ or $g'_k(t) \leq 0$ for all $t \in \mathbb{E}$. This property allows us to formulate the following theorem.

Theorem 1: Let $\mathcal{E} \subset \mathcal{U}$ be parameterized by a vector-function $\mathbf{g} : \mathbb{E} \to \mathcal{E}$. Let the following two conditions be satisfied:

$$g'_k(t) \geq 0, k = 1, 2 \text{ for all } t \in \mathbb{E}, \tag{29a}$$

$$T(\mathbf{I}_d) \begin{cases} \geq 0 \text{ for } \mathbf{I}_d \in \mathcal{G}_1, \\ \leq 0 \text{ for } \mathbf{I}_d \in \mathcal{G}_2, \end{cases} \tag{29b}$$

where the regions $\mathcal{G}_k$, $k = 1, 2$ are defined as $\mathcal{G}_1 \equiv \big\{\mathbf{I}_d : I_{d,1} \leq g_1(t), I_{d,2} \geq g_2(t), \forall t \in \mathbb{E}\big\}$ and $\mathcal{G}_2 \equiv \big\{\mathbf{I}_d : I_{d,1} \geq g_1(t), I_{d,2} \leq g_2(t), \forall t \in \mathbb{E}\big\}$. Then, the convergence curve

$$\mathcal{S} = \mathcal{E} \cup \mathcal{L}(a_0, \mathbf{g}(0)) \cup \mathcal{L}(\mathbf{g}(1), a_2) \tag{30}$$

[4]Note that extensive simulations show that using a 2D quadratic form gives a close approximation to $f_{e,k}$. Note also that a polynomial approximation on the EXIT functions has been used in [8] to design LDPC codes for iterative MIMO systems.

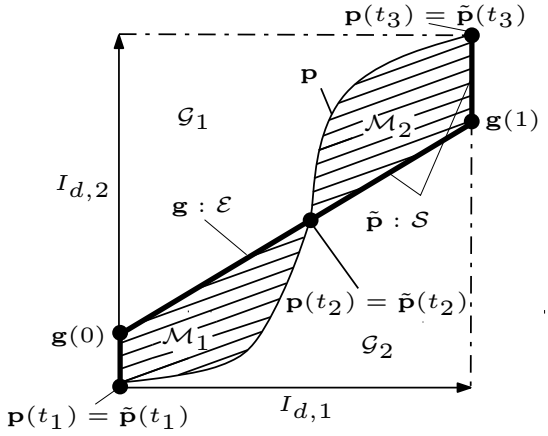

Fig. 4. Curve $\mathbf{g} : \mathcal{E}$, corresponding convergence curve $\tilde{\mathbf{p}} : \mathcal{S}$, and partition of $\tilde{\mathbf{p}}$ for an arbitrary parametric curve $\mathbf{p} \in \mathcal{P}$ in the plane region $\mathcal{U}$.

comprised of the curve $\mathcal{E}$ and the two straight line segments (all shown in Fig. 4) is optimal with respect to (22).

The following proof of *Theorem 1* is based on Green's theorem [18] and is similar to that presented in [19].

Proof: For any admissible parametric curve $\mathbf{p} \in \mathcal{P}$, we can find a parameterization $\tilde{\mathbf{p}} \in \mathcal{P}$ of $\mathcal{S}$ and a partitioning $\bigcup_i [t_i, t_{i+1}]$ of the interval $\mathbb{E}$ such that for each interval $[t_i, t_{i+1}]$, one has $\mathbf{p}(t_i) = \tilde{\mathbf{p}}(t_i)$, $\mathbf{p}(t_{i+1}) = \tilde{\mathbf{p}}(t_{i+1})$, and $\mathbf{p}(t) \in \mathcal{G}_1$ or $\mathbf{p}(t) \in \mathcal{G}_2$, for all $t \in [t_i, t_{i+1}]$. An example of such a partitioning is shown in Fig. 4. Based on the partitioning, we can express the sum rate difference $R[\tilde{\mathbf{p}}] - R[\mathbf{p}]$ between $\tilde{\mathbf{p}}$ and $\mathbf{p}$ as

$$R[\tilde{\mathbf{p}}] - R[\mathbf{p}] = \sum_i \left(\Delta R_i \equiv \int_{t_i}^{t_{i+1}} Y(\tilde{\mathbf{p}}) \mathrm{d}t - \int_{t_i}^{t_{i+1}} Y(\mathbf{p}) \mathrm{d}t \right). \tag{31}$$

Each increment ΔR_i can be written as line integral along the closed curve $\mathcal{A}_i \equiv \{\mathbf{p}(t), \tilde{\mathbf{p}}(t) : t \in [t_i, t_{i+1}]\}$ yielding

$$\Delta R_i = \gamma_i \oint_{\mathcal{A}_i} f_{e,1}(\mathbf{I}_d) \mathrm{d}I_{d,1} + \gamma_i \oint_{\mathcal{A}_i} f_{e,2}(\mathbf{I}_d) \mathrm{d}I_{d,2}, \tag{32}$$

where $\gamma_i = 1$ when $\mathbf{p}(t) \in \mathcal{G}_1$, for all $t \in [t_i, t_{i+1}]$, and $\gamma_i = -1$ otherwise. Let each simple closed curve $\mathcal{A}_i$ be oriented in the positive direction with the bounded region $\mathcal{M}_i \subseteq \mathcal{U}$ on the left. Then, applying Green's theorem to (32) allows us to rewrite ΔR_i as

$$\Delta R_i = \gamma_i \iint_{\mathcal{M}_i} T(\mathbf{I}_d) \mathrm{d}I_{d,1} \mathrm{d}I_{d,2}. \tag{33}$$

With the conditions in (29), we can state that $\Delta R_i \geq 0$ since either $\mathcal{M}_i \subseteq \mathcal{G}_1$ or $\mathcal{M}_i \subseteq \mathcal{G}_2$, as shown in Fig. 4. Thus, we conclude that $R[\tilde{\mathbf{p}}] \geq R[\mathbf{p}]$ for any $\mathbf{p} \in \mathcal{P}$, which yields the optimality of $\mathcal{S}$ in (30). ■

The optimality of $\mathcal{S}$ in (30) is given only when both conditions (29) are satisfied. In the cases when at least one of these conditions is violated, we can use Green's theorem as in (31) and (32) to show that *candidate solutions* to problem (22) are the convergence curves $\mathcal{H}_0(u) \equiv \mathcal{L}(a_0, r_{0,1}, r_{0,2}, a_2)$ and $\mathcal{H}_1(u) \equiv \mathcal{L}(a_0, r_{1,1}, r_{1,2}, a_2)$, which are comprised of the union of three straight-line segments connecting the points $r_{0,1} = (u, 0)$, $r_{0,2} = (u, 1)$ and $r_{1,1} = (0, u)$, $r_{1,2} = (1, u)$ with $u \in \mathbb{E}$. Using the candidate solutions, we show in Appendix B that problem (22) can be rewritten as a quadratic extremal problem, which may be solved with standard methods of classical calculus [18].

The three possible outcomes of (28) discussed above, can now be used to calculate the convergence curve that solves problem (22), which is summarized in Algorithm 1.

Algorithm 1 Algorithm for computing the convergence curve that maximizes the sum rate

1: Calculate the coefficients in (27) for each EQ EXIT function $f_{e,k}$ using a standard regression method [18].
2: **if** (45) is satisfied **then**
3: Output the boundary curve that solves (46).
4: **else if** (45a) is satisfied and (45b) is violated **then**
5: Output an arbitrary convergence curve $\mathbf{p} \in \mathcal{P}$.
6: **else if** (29) is satisfied **then**
7: Output the convergence curve in (30).
8: **else**
9: Output the convergence curve $\mathcal{H}_l(u)$, $l = 1, 2$, $u \in \mathbb{E}$ with (l, u) being the solution to (51).
10: **end if**

C. Rate Allocation using EXIT Functions

Let $\bar{\mathbf{p}} \in \mathcal{P}$ be the convergence curve that solves problem (22). An upper bound of the rate of user k with respect to $\bar{\mathbf{p}}$ is then given by the area under the EXIT function $f_k^{(\bar{\mathbf{p}})}$, $R_k = \int_0^1 f_k^{(\bar{\mathbf{p}})}(I_{d,k}) \mathrm{d}I_{d,k}$, as illustrated in Fig. 2. To closely approach the rate R_k, the code of user k should have its DEC EXIT function $f_{d,k}$ as close to $f_k^{(\bar{\mathbf{p}})}$ as possible, while satisfying the constraints in (10). In practice, however, optimizing $f_{d,k}$ by adjusting the available code parameters such that optimality in a strict sense is guaranteed may not be possible, since the code parameters are presumably limited. Thus, for practical reasons, we restrict each transmitter to have only a finite set of codes $\mathcal{C} = \{C_1, ..., C_m\}$, with m being the number of the codes in the set, with fixed rates. Then, a simple approach for rate allocation is to *select*, for each k, the code $C_n \in \mathcal{C}$ with the highest possible rate at which convergence is achieved, while its DEC EXIT function $f_{d,k}^{(C_n)}$ best fits to $f_k^{(\bar{\mathbf{p}})}$. Based on this concept, we now propose a rate allocation algorithm, which is summarized as follows.

1) For each realization of the FD channel matrices ($\mathbf{\Xi}_1$, $\mathbf{\Xi}_2$), calculate the EQ EXIT functions $f_{e,1}$ and $f_{e,2}$ using (8).
2) Calculate the convergence curve $\bar{\mathbf{p}} \in \mathcal{P}$ that solves (22) using Algorithm 1.
3) Calculate $f_k^{(\bar{\mathbf{p}})}$ by projecting the space curve $\mathbf{w}_k(\bar{\mathbf{p}})$ onto the $I_{e,k}$-$I_{d,k}$-plane.
4) To obtain high information rate, select the channel code for each user that satisfies:

$$r_{c,k} = \max_{C_n \in \mathcal{C}} \Big\{ r(C_n) : f_k^{(\bar{\mathbf{p}})}(I_{d,k}) \geq f_{d,k}^{(C_n)}(I_{d,k}) + z(I_{d,k}), \forall I_{d,k} \in [0, 1) \Big\}, \tag{34}$$

where $r(C_n)$ denotes the rate of code C_n, and $z(I_{d,k})$ is a function to control the speed of convergence of the decoding trajectory to the maximum point $\mathbf{I}_d^* = a_2$.

5) If $r_{c,k}$ is NULL, select the code with the lowest possible rate in $\mathcal{C}$,

$$r_{c,k} = \min_{C_n \in \mathcal{C}} r(C_n). \tag{35}$$

6) Output the selected coding rates $r_{c,1}$ and $r_{c,2}$.

D. Outage-based Rate Allocation

In this section, we extend the above *code selection* algorithm to an outage-based rate allocation approach for non-ergodic fading channels. In the context of turbo equalization, the coding rate $r_{c,k}$ of the k-th user should be no greater than $r_{c,k}^*(\bar{\mathbf{p}}) \equiv \max_{C_n \in \mathcal{C}} \{r(C_n) : f_k^{(\bar{\mathbf{p}})}(I_{d,k}) \geq f_{d,k}^{(C_n)}(I_{d,k}) + z(I_{d,k}), \forall I_{d,k} \in [0,1)\}$ with $\bar{\mathbf{p}} \in \mathcal{P}$ being the solution to (22), such that the constraints in (10) are satisfied. Assume that for each code $C_n \in \mathcal{C}$ we have $f_d^{(C_n)}(I_d) \geq f_d^{(C_m)}(I_d)$, for all $I_d \in [0,1)$ if $r(C_n) \geq r(C_m)$ with $C_m \in \mathcal{C}$. Then, the set of code rate pairs, at which convergence of turbo equalization is achieved for the specific FD channel matrices ($\boldsymbol{\Xi}_1$, $\boldsymbol{\Xi}_2$), is given by

$$\mathcal{T}(\bar{\mathbf{p}}) \equiv \big\{(r_{c,1}, r_{c,2}) : r_{c,1} = r(C_n) \leq r_{c,1}^*(\bar{\mathbf{p}}), \; r_{c,2} = r(C_m) \leq r_{c,2}^*(\bar{\mathbf{p}}), C_n, C_m \in \mathcal{C}\big\}. \tag{36}$$

For an outage-based rate allocation, we view the rate pair $\big(r_{c,1}^*(\bar{\mathbf{p}}), r_{c,2}^*(\bar{\mathbf{p}})\big)$ as random variables since $\bar{\mathbf{p}}$ depends on ($\boldsymbol{\Xi}_1$, $\boldsymbol{\Xi}_2$) which are random matrices whose particular realizations change independently, frame-by-frame. If the two users are transmitting at rates $(r_{c,1}, r_{c,2})$, an outage event occurs if either $r_{c,1} > r_{c,1}^*(\bar{\mathbf{p}})$ or $r_{c,2} > r_{c,2}^*(\bar{\mathbf{p}})$. Thus, we define the outage probability for the code rate pair $(r_{c,1}, r_{c,2})$ as $P_{out}(r_{c,1}, r_{c,2}) \equiv \text{Prob}\big((r_{c,1}, r_{c,2}) \notin \mathcal{T}(\bar{\mathbf{p}})\big)$. The 2-user outage rate region is then given by

$$\mathcal{R}_\epsilon^{out} \equiv \big\{(r_{c,1}, r_{c,2}) : P_{out}(r_{c,1}, r_{c,2}) \leq \epsilon\big\}, \tag{37}$$

where ϵ denotes the outage probability. The maximum sum rate at which reliable transmission for the two users is possible for $(1-\epsilon)\cdot 100\%$ of the channel realizations, can then be expressed as solution to the problem:

$$R_\epsilon^{out} = \max_{(r_{c,1}, r_{c,2}) \in \mathcal{R}_\epsilon^{out}} r_{c,1} + r_{c,2}. \tag{38}$$

For the prescribed constraint $P_{out}(r_{c,1}, r_{c,2}) \leq \epsilon$, the coding rates ($r_{c,1}$, $r_{c,2}$) satisfying (38) are the largest rates over the 2-user MAC for the given codes in $\mathcal{C}$. In this paper, we obtain the region in (37) by a Monte Carlo method, as described in Section V-C.

V. Numerical Results

In this section, results of capacity calculations and simulations conducted to evaluate the throughput enhancement achieved by the proposed two rate allocation approaches are presented. We consider a single-carrier block-cyclic transmission over frequency-selective Rayleigh block-fading channels,

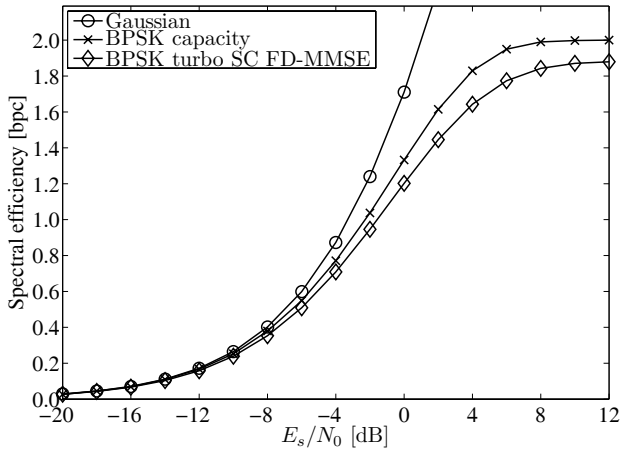

Fig. 5. Spectral efficiency of a 2-user turbo system with SC FD-MMSE equalization when optimally designed user codes are assumed for transmission, and ergodic sum capacity with Gaussian and with BPSK inputs. $Q = 32$, $L = 3$, $P = 2$.

where typical values of L ($L = 3$, $L = 5$ and $L = 32$) are assumed. We define the average SNR at the receiver as

$$\frac{E_s}{N_0} \equiv \frac{\sum_{m=1}^{M} \sum_{l=0}^{L-1} \mathrm{E}\big[|h_{k,m}(l)|^2\big] E_0}{M\sigma^2}, \tag{39}$$

where E[·] denotes expectation, and E_0 is the total energy per symbol at the transmitters.

A. Maximum Spectral Efficiency

Fig. 5 shows the maximum achievable spectral efficiency $\rho \equiv \frac{Q}{Q+P}\tilde{R}$ of the 2-user turbo system, when assuming (optimally designed) user codes whose DEC EXIT functions satisfy:

$$f_{d,k} = f_k^{(\bar{\mathbf{p}})}, \text{ for } k = 1, 2. \tag{40}$$

In (40), $\bar{\mathbf{p}}$ is the solution to problem (22) for a specific channel realization given. The rate $\tilde{R}$ has been calculated by averaging $R = \sum_{k=1}^{2} \int_0^1 f_k^{(\bar{\mathbf{p}})}(I_{d,k}) \mathrm{d}I_{d,k}$ over a large number of channel realizations. For comparison, the ergodic i.i.d. Gaussian-input sum capacity [20] and the ergodic BPSK-input sum capacity of the frequency-selective Rayleigh fading channel ($L = 3$) with evenly allocated transmit power are also shown. The BPSK-input capacity result has been obtained by a Monte Carlo method, as described in [21]. We assume that the channel state information is known only at the receiver. Comparing the numerical results in Fig. 5, we find that the loss incurred by the use of SC FD-MMSE equalization with respect to the BPSK-input capacity slightly increases for large values of E_s/N_0. We also observe that there is almost no difference between the three curves up to $E_s/N_0 = -8$ dB, indicating that the 2-user turbo system with BPSK-inputs, using SC FD-MMSE equalization with user codes whose DEC EXIT functions satisfy (40), is nearly optimal in the low E_s/N_0 region.

B. Rate Allocation with Practical Codes

The rate-compatible punctured SCCCs proposed in [22], consisting of a rate-r_c outer encoder and a recursive rate-

TABLE I
SELECTED CODE RATE PAIRS AND INFORMATION RATE PAIRS OF BOTH USERS FOR TWO DIFFERENT CONVERGENCE CURVES.

	$r_{c,1}$	$r_{c,2}$	r_c	R_1	R_2	R
Max-Sum-Rate	0.75	0.85	1.60	0.84	0.90	1.74
Min-Sum-Rate	0.90	0.45	1.35	0.98	0.58	1.56

1 inner encoder with polynomials $(g_r, g_0) = (3, 2)$ (g_r denotes the feedback polynomial) in octal notation, are assumed for rate allocation at both users. The outer encoder of the SCCC is selected from a set of 17 subcodes with rates $r_c = 0.05 \cdot (1 + n)$, $n = 1, .., 17$. The length of a frame is fixed to $NQ = 16384$ BPSK symbols, and $z(x)$ in (34) is defined as $z(x) = 0.025 - 0.025x$. The turbo EQ performs 15 iterations between the EQ and both SCCC DECs, and 20 iterations between the inner and outer DEC. Note that $z(x)$ is preliminarily optimized by computer simulations to find an acceptable trade-off between performance of the turbo EQ and number of iterations needed to ensure convergence.

Table I shows the selected code rate pairs at $E_s/N_0 = 4.75$ dB with respect to (34) and the information rate pairs satisfying (22) for a single random channel realization. The channel coefficients are given by $h_{1,1} = [0.045 + 0.027i, -0.054 + 0.045i, -0.134 - 0.022i]^T$, $h_{1,2} = [-0.124 + 0.125i, -0.038 - 0.010i, -0.193 + 0.590i]^T$, $h_{2,1} = [-0.042 + 0.020i, -0.140 - 0.036i, -0.145 - 0.121i]^T$, and $h_{2,2} = [-0.157 + 0.186i, -0.153 + 0.078i, 0.198 + 0.312i]^T$ with $i = \sqrt{-1}$. For comparison, the selected code rate pairs $r_{c,k}$ and information rate pairs $R_k = \int_{\check{\mathbf{p}}} f_{e,k}(\mathbf{I}_d)\mathrm{d}I_{d,k}$, computed for the convergence curve satisfying $\check{\mathbf{p}} \equiv \arg\min_{\mathbf{p}\in\mathcal{P}} \sum_{k=1}^{2} \int_{\mathbf{p}} f_{e,k}(\mathbf{I}_d)\mathrm{d}I_{d,k}$, are also shown and referred to as 'Min-Rate-Sum'. The results in Table I indicate that the selected code rate pairs of both users, and thus the total achievable rate of the turbo system, strongly depend on the convergence curve chosen for the particular channel realization.

Fig. 6 shows the BER performance of the turbo EQ for a single channel realization having the same coefficients as given above. The users' codes are selected with respect to (34) at SNR $E_s/N_0 = 4.75$ dB. Also shown is the SNR $E_s/N_0|_{\min}$ at which the *instantaneous* BPSK-input sum capacity (for the given channel realization) is equal to the total rate $\sum_{k=1}^{2} r_{c,k} = 1.60$ bit per channel use (bpc) of the turbo system. It is observed that the selected codes show convergence starting at 3.6 dB and 4.1 dB E_s/N_0 for user 1 and user 2, respectively. Thus, the SC FD-MMSE turbo EQ indeed satisfies the convergence constraints (10) for the desired SNR $E_s/N_0|_{\mathrm{des}}$. Further, we observe that the turbo EQ operates within about 2 dB E_s/N_0 to its respective capacity limit at a BER of 10^{-6}.

For evaluating the throughput efficiency, a selective-repeat automatic repeat-request (ARQ) system with infinite buffering [23] is assumed. Fig. 7 shows the average total throughput of the turbo system versus E_s/N_0 for $L = 32$ channels. The spectral efficiency ρ (see Section V-A) of the turbo system with user codes whose DEC EXIT functions satisfy (40), is shown as a reference. Also shown is the average total throughput performance for an ARQ scheme with fixed coding rates $r_{c,1/2} = 0.1 \cdot n$, $n = 1, .., 9$ of both users. As observed

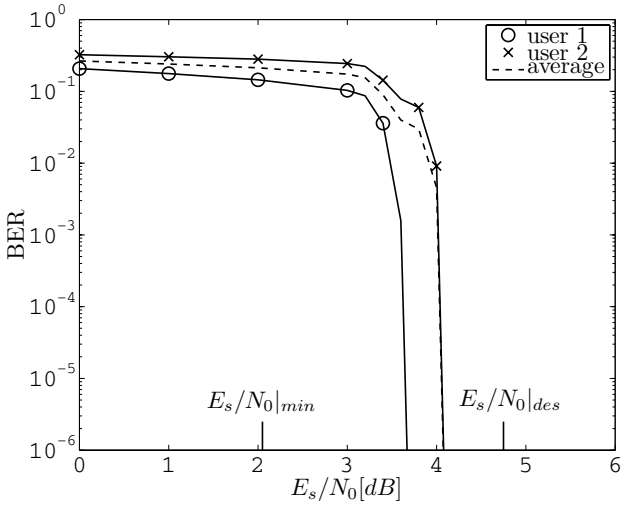

Fig. 6. BER performance of the turbo EQ for a fixed $L = 3$ channel realization with user codes having the coding rates $r_{c,1} = 0.75$ and $r_{c,2} = 0.85$. $Q = 32$, $L = 3$.

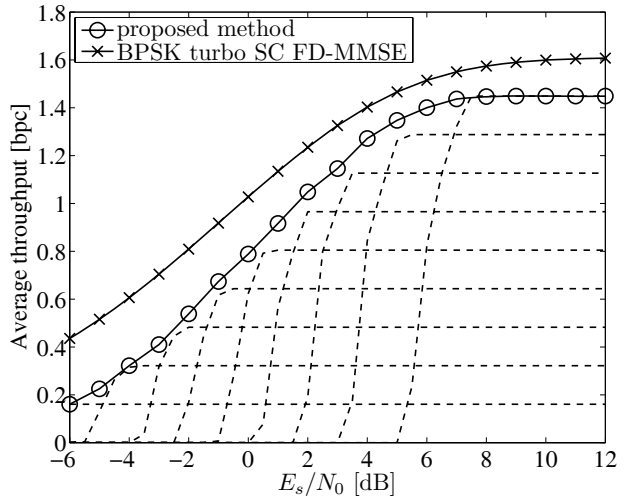

Fig. 7. Average total throughput of both users versus E_s/N_0 for the proposed rate allocation scheme and for ARQ with fixed coding rates $r_{c,1/2} = 0.1 \cdot n$ with $n = 1, .., 9$ (dashed curves, from bottom to top). $Q = 128$, $L = 32$.

in Fig. 7, substantial throughput gain is obtained with the rate allocation approach proposed in Section IV-C over fixed rate ARQ. Further, we find that the throughput performance is only 1.5 dB away (in the high E_s/N_0 region) from the throughput achieved when optimally designed user codes are assumed for transmission. Notably, however, there is still a gap of almost 2.5 dB between both curves in the low E_s/N_0 region. It should be noted though, that by using more flexible coding techniques, such as irregular SCCCs (e.g., see [22]) or irregular LDPC codes (e.g., see [8]) which allow a code design, given the channel realizations, the performance loss can be reduced.

C. Outage-based Rate Allocation and Outage Capacity Region

In this section, the outage-based rate allocation technique proposed in Section IV-D is applied to $L = 5$ channels. The same code set as in Section V-B is assumed for rate allocation

TABLE II
CODE RATE PAIRS AND ACHIEVABLE INFORMATION RATES OF A 2-USER SYSTEM WITH BPSK INPUTS FOR OUTAGE PROBABILITY OF $\epsilon = 0.1$.

E_s/N_0 [dB]	$r_{c,1}$	$r_{c,2}$	r_c	$\hat{r}_1$	$\hat{r}_2$	$\hat{r}$
0	0.35	0.35	0.70	0.47	0.53	1.00
1	0.40	0.40	0.80	0.55	0.61	1.16
2	0.50	0.50	1.00	0.64	0.67	1.31
3	0.55 0.60	0.60 0.55	1.15	0.70	0.76	1.46
4	0.65	0.65	1.30	0.79	0.82	1.61

at both users. In addition, we include the numerical results for the boundary calculation for the outage binary-input capacity region [24], [25] with various values of outage probabilities as references. The outage binary-input capacity region of the 2-user MAC is defined as the set of all rate pairs (r_1, r_2) satisfying [24]

$$\mathcal{C}_\epsilon^{out} \equiv \big\{(r_1, r_2) : P_o(r_1, r_2) \leq \epsilon\big\}, \tag{41}$$

where $P_o(r_1, r_2) \equiv \text{Prob}\big((r_1, r_2) \notin \mathcal{C}_b(\Xi_1, \Xi_2)\big)$ is the outage probability constraint for the rate pair (r_1, r_2) with $\mathcal{C}_b(\Xi_1, \Xi_2)$ being the binary-input capacity region conditioned on the specific FD channel realization (Ξ_1, Ξ_2). The binary-input capacity region $\mathcal{C}_b(\Xi_1, \Xi_2)$ can be expressed as follows [12]:

$$\mathcal{C}_b(\Xi_1, \Xi_2) \equiv \big\{(r_1, r_2) : \sum_{k \in \mathcal{Z}} r_k \leq \text{I}(\mathbf{r}; b_k, k \in \mathcal{Z} \,|b_l, l \in \bar{\mathcal{Z}})\big\}, \tag{42}$$

where $\mathcal{Z}$ denotes any subset of $\{1, 2\}$, and $\bar{\mathcal{Z}}$ its complement[5]. Fig. 8 shows the code rate pairs $(r_{c,1}, r_{c,2})$ that maximize sum rate among those combinations of the codes in the code set $\mathcal{C}$ for outage probabilities $\epsilon = 0.01$, 0.1, and 0.5. In all the cases, the E_s/N_0 is set at 4 dB. To obtain the code rate pairs for the outage constraint $P_{out}(r_{c,1}, r_{c,2}) \leq \epsilon$, we computed the 2-user outage rate region $\mathcal{R}_\epsilon^{out}$ by transmitting over V independent channel realizations. Specifically, we determined the set of code rate pairs $\mathcal{T}(\bar{\mathbf{p}})$ for each of the V channel realizations according to (36), and recorded the total number U of outage events $((r_{c,1}, r_{c,2}) \notin \mathcal{T}(\bar{\mathbf{p}}))$ for a given code rate pair $(r_{c,1}, r_{c,2})$. According to the definition of $\mathcal{R}_\epsilon^{out}$, all the code rate pairs $(r_{c,1}, r_{c,2}) \in \mathcal{R}_\epsilon^{out}$ satisfy the condition $\frac{U}{V} \leq \epsilon$, and the code rate pairs that maximize sum rate can easily be computed with (38). Also shown in Fig. 8 are the outage binary-input capacity regions $\mathcal{C}_\epsilon^{out}$ for the three different values of ϵ, obtained by a Monte Carlo method [21]. The achievable rate pairs on the region boundaries that maximize outage capacity, i.e., $(\hat{r}_1, \hat{r}_2) = \max_{(r_1, r_2) \in \mathcal{C}_\epsilon^{out}} r_1 + r_2$ are marked as well. As it is evident from this figure, the larger the desired outage probability, the larger is the resulting outage binary-input capacity region. Furthermore, as expected, the code rate pairs that satisfy (38) are contained by their respective outage binary-input capacity region. We observe that these rate pairs are almost symmetric with respect to the line $r_1 = r_2 = R_\epsilon^{out}/2$. This is apparently obvious since we expect that the two users' rates obtained by (22) are equal in the sense of average. Note that, due to a finite number of Monte Carlo trials, the rate pairs are not exactly symmetric. The code rate pairs for a given outage probability of $\epsilon = 0.1$ at different E_s/N_0-values are listed in Table II.

[5]Note that the indices n and q in the variable $b_{q,k}(n)$ have been omitted in (42) for notational simplicity.

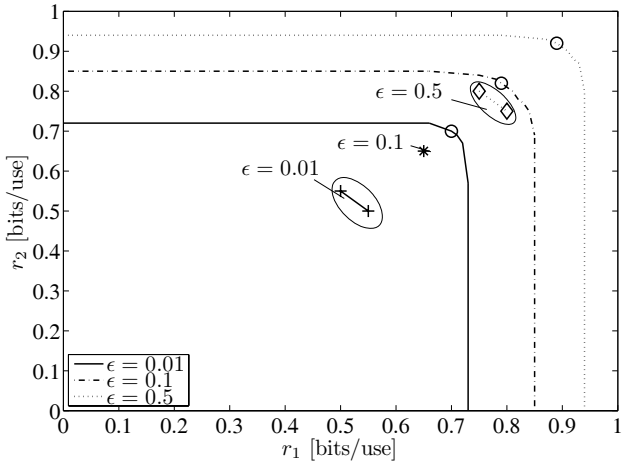

Fig. 8. Achievable code rate pairs (markers: '+', '$*$', and '$\diamond$') for the two users that maximize sum rate for the given code set $\mathcal{C}$ and respective 2-user outage binary-input capacity regions when $\epsilon = 0.01$, 0.1, 0.5, and $E_s/N_0 = 4$ dB. The 'o' markers indicate the achievable rates of the two users that maximize outage capacity with the desired outage probability.

For comparison, the maximal achievable rates $(\hat{r}_1, \hat{r}_2)$ are also listed. As observed in Table II, there is still a performance loss of about 0.3 bpc in sum rate over the considered E_s/N_0 range of the proposed outage-based rate allocation approach, compared to the outage capacity results. Reducing this loss by using appropriate but still practical coding techniques is an interesting further research topic that will be considered in our future work.

VI. CONCLUSION

In this paper, we consider the problem of rate allocation in frequency-selective 2-user Gaussian multiple access fading channels employing SC FD-MMSE turbo equalization. The area property theorem for EXIT charts is used to derive an upper bound on the rate region of the turbo system. Using this bound, we study the problem of maximizing the sum rate of both users, given the EXIT function of the EQ, and present an approximate solution to this optimization problem. In addition, a simple code selection algorithm for rate allocation, using the EXIT curves obtained as a result of the sum rate optimization, is proposed. Numerical results show that the achievable throughput of the proposed algorithm using rate-compatible punctured SCCCs for each user, is only 1.5 dB away for high E_s/N_0 from the maximal supportable throughput achieved with optimally designed user codes for each channel realization. Furthermore, the extension of this algorithm to an outage-based rate allocation approach is discussed. It should be emphasized here that the proposed two algorithms are only applicable for the 2-user case. In [26], the authors discuss a heuristic approach based on a dynamic programming principle that extends the proposed algorithms to more generic cases having more than two users.

APPENDIX A

Using (27), the functional in (23) can be written as

$$\int_0^1 Y(\mathbf{p})\mathrm{d}t \approx c + \int_0^1 h_1(p_1)p_2'\mathrm{d}t + \int_0^1 h_2(p_2)p_1'\mathrm{d}t, \tag{43}$$

where $h_1(p_1) \equiv \alpha_{2,1}p_1 + (\alpha_{2,4} - \alpha_{1,3}/2)p_1^2$ and $h_2(p_2) \equiv \alpha_{1,2}p_2 + (\alpha_{1,5} - \alpha_{2,3}/2)p_2^2$ are quadratic polynomials in p_1 and p_2, respectively, and c is a constant. The Euler-Lagrange equation in (28) can be written with (27) as

$$\alpha_{2,1} - \alpha_{1,2} + (2\alpha_{2,4} - \alpha_{1,3})I_{d,1} - (2\alpha_{1,5} - \alpha_{2,3})I_{d,2} \stackrel{!}{=} 0. \tag{44}$$

In the case when (28) has no solution, the coefficients of the polynomials $h_1(p_1)$ and $h_2(p_2)$ satisfy:

$$\alpha_{1,3} = 2\alpha_{2,4}, \alpha_{2,3} = 2\alpha_{1,5}, \tag{45a}$$

$$\alpha_{2,1} - \alpha_{1,2} \neq 0. \tag{45b}$$

By (43) and (45), the variational problem in (22) becomes

$$R_{max} \approx c + \max_{\mathbf{p}\in\mathcal{P}} \Big\{ (\alpha_{1,2} - \alpha_{2,1}) \int_{\mathbf{p}} I_{d,2} \mathrm{d}I_{d,1} \Big\}. \tag{46}$$

Now, it is easy to confirm that the sum rate expression given by (46) is maximized, either for $\mathbf{p}(t) \in \mathcal{L}(a_0, a_1, a_2)$, for all $t \in \mathbb{E}$ if $\alpha_{1,2} > \alpha_{2,1}$ or $\mathbf{p}(t) \in \mathcal{L}(a_0, a_3, a_2)$, for all $t \in \mathbb{E}$ if $\alpha_{1,2} < \alpha_{2,1}$.

APPENDIX B

Using the integral expression in (43), we can express the sum rates $R_0(u)$ and $R_1(u)$ for $\mathcal{H}_0(u)$ and $\mathcal{H}_1(u)$, respectively, as functions of $u \in \mathbb{E}$, as

$$R_0(u) \equiv c + \int_0^u h_2(0)\mathrm{d}I_{d,1} + \int_0^1 h_1(u)\mathrm{d}I_{d,2} + \int_u^1 h_2(1)\mathrm{d}I_{d,1}, \tag{47}$$

$$R_1(u) \equiv c + \int_0^u h_1(0)\mathrm{d}I_{d,2} + \int_0^1 h_2(u)\mathrm{d}I_{d,1} + \int_u^1 h_1(1)\mathrm{d}I_{d,2}, \tag{48}$$

Integrating each term in (47) and (48) allows us to rewrite $R_0(u)$ and $R_1(u)$ as

$$R_0(u) = c + h_1(u) + (1-u)h_2(1), \tag{49}$$

$$R_1(u) = c + h_2(u) + (1-u)h_1(1). \tag{50}$$

Thus, the variational problem in (22) reduces to:

$$R_{max} \approx \max_{l\in\{0,1\}} \max_{u\in[0,1]} \{R_l(u)\}, \tag{51}$$

of which solution can easily be obtained with the standard framework of classical calculus, since the objective function is quadratic in u [18].

REFERENCES

[1] C. Douillard, *et al.*, "Iterative correction of intersymbol interference: turbo equalization," *European Trans. Telecommun.*, vol. 6, no. 5, pp. 507-511, Sept. 1995.

[2] X. Wang and H. V. Poor, "Iterative (turbo) soft interference cancellation and decoding for coded CDMA," *IEEE Trans. Commun.*, vol. 47, no. 7, pp. 1046-1061, July 1999.

[3] M. Tüchler and J. Hagenauer, "Turbo equalization: principles and new results," *IEEE Trans. Commun.*, vol. 50, no. 5, pp. 754-767, May 2002.

[4] T. Abe and T. Matsumoto, "Space-time turbo equalization in frequency-selective MIMO channels," *IEEE Trans. Veh. Technol.*, vol. 52, no. 3, pp. 469-475, May 2003.

[5] K. Kansanen and T. Matsumoto, "An analytical method for MMSE MIMO turbo equalizer EXIT chart computation," *IEEE Trans. Wireless Commun.*, vol. 6, no. 1, pp. 59-63, Jan. 2007.

[6] S. ten Brink, "Convergence behavior of iteratively decoded parallel concatenated codes," *IEEE Trans. Commun.*, vol. 49, no. 10, pp. 1727-1737, Oct. 2001.

[7] A. Ashikhmin, G. Kramer, and S. ten Brink, "Extrinsic information transfer functions: model and erasure channel properties," *IEEE Trans. Inf. Theory*, vol. 50, no. 11, pp. 2657-2673, Nov. 2004.

[8] S. ten Brink, G. Kramer, and A. Ashikhmin, "Design of low-density parity-check codes for modulation and detection," *IEEE Trans. Commun.*, vol. 52, no. 4, pp. 670-678, Apr. 2004.

[9] S. ten Brink and G. Kramer, "Design of repeat-accumulate codes for iterative detection and decoding," *IEEE Trans. Signal Process.*, vol. 51, no. 11, pp. 2764-2772, Nov. 2003.

[10] A. Roumy and D. Declercq, "Characterization and optimization of LDPC codes for the 2-user Gaussian multiple access channel," *EURASIP J. Wireless Commun. and Netw.*, vol. 2007, Article ID 74890, 10 pages, 2007.

[11] A. Amraoui, S. Dusad, and R. Urbanke, "Achieving general points in the 2-user Gaussian MAC without time-sharing or rate-splitting by means of iterative coding," in *Proc. IEEE Int. Symp. Inf. Theory*, Lausanne, Switzerland, July 2002.

[12] T. M. Cover and J. A. Thomas, *Elements of Information Theory*. New York: John Wiley &. Sons, Inc., 1991.

[13] B. Rimoldi and R. Urbanke, "A rate-splitting approach to the Gaussian multiple-access channel," *IEEE Trans. Inf. Theory*, vol. 42, no. 2, pp. 364-375, Mar. 1996.

[14] A. Sanderovich, M. Peleg, and S. Shamai (Shitz), "LDPC coded MIMO multiple access with iterative joint decoding," *IEEE Trans. Inf. Theory*, vol. 51, no. 4, pp. 1437-1450, Apr. 2005.

[15] C. Schlegel, Z. Shi, and M. Burnashev, "Optimal power/rate allocation and code selection for iterative joint detection of coded random CDMA," *IEEE Trans. Inf. Theory*, vol. 52, no. 9, pp. 4286-4294, Sept. 2006.

[16] F. Brännström, L. K. Rasmussen, and A. J. Grant, "Convergence analysis and optimal scheduling for multiple concatenated codes," *IEEE Trans. Inf. Theory*, vol. 51, no. 9, pp. 3354-3364, Sept. 2005.

[17] J. Jost and X. Li-Jost, "Calculus of variations," *Cambridge Studies in Advanced Mathematics*, vol. 64. Cambridge University Press, 1998.

[18] E. Kreyszig, *Advanced Engineering Mathematics*, 9th ed. New York: John Wiley & Sons, 2005.

[19] A. Miele, "Extremization of linear integrals by Green's theorem," *Optimization Technics*, G. Leitmann Ed. New York: Academic Press, pp. 69-98, 1962.

[20] W. Rhee and J. M. Cioffi, "Ergodic capacity of multiantenna Gaussian multiple-access channels," in *Proc. 35th Asilomar Conf. Signals, Systems, Computers*, vol. 1, pp. 507-512, Nov. 2001.

[21] Z. Zhang *et al.*, "Achievable information rates and coding for MIMO systems over ISI channels and frequency-selective fading channels," *IEEE Trans. Commun.*, vol. 52, no. 10, pp. 1698-1710, Oct. 2004.

[22] M. Tüchler, "Design of serially concatenated systems depending on the block length," *IEEE Trans. Commun.*, vol. 52, no. 2, pp. 209-218, Feb. 2004.

[23] K. Kansanen *et al.*, "Multilevel-coded QAM with MIMO turbo-equalization in broadband single-carrier signaling," *IEEE Trans. Veh. Technol.*, vol. 54, no. 3, pp. 954-966, May 2005.

[24] J. Haipeng and A. Acampora, "Bounds on the outage-constrained capacity region of space-division multiple-access radio systems," *EURASIP J. Appl. Signal Proc.*, vol. 2004, no. 9, pp. 1288-1298, 2004.

[25] T. Guess, H. Zhang, and T.V. Kotchiev, "The outage capacity of BLAST for MIMO channels," in *Proc. IEEE Conf. Commun.*, vol. 4, pp. 2628-2632, May 2003.

[26] M. Grossmann and T. Matsumoto, "Rate allocation for K-user MAC with turbo equalization," in *Proc. International ITG Workshop Smart Antennas 2009*, vol. 1, pp. 281-288, Feb. 2009.

Marcus Grossmann received the Diplom-Ingenieur (M.S.) degree in electrical engineering and computer science, from Ilmenau University of Technology, Germany, in 2004. He is currently working towards the Ph.D. degree at the same university. His research interests are in the area of communication systems, and signal processing for wireless communications.

Thomas Ortlepp received the Dipl.-Math. degree in mathematics from Ilmenau University of Technology, Germany, in 1999. He moved to the Institute of Information Technology and received the Dr.-Ing. degree in electrical engineering in 2004. T. Ortlepp works as a lecturer for electromagnetics, relativistic electrodynamics and superconductive electronics. His main research interest is mixed signal circuit analysis with main focus on circuit simulation, design, analysis of noise induced errors, and jitter as well as new circuit topologies.

Tad Matsumoto (S'84, SM'95) received his B.S., M.S., and Ph.D. degrees from Keio University, Yokohama, Japan, in 1978, 1980, and 1991, respectively, all in electrical engineering. He joined Nippon Telegraph and Telephone Corporation (NTT) in April 1980. Since he engaged in NTT, he was involved in a lot of research and development projects, all for mobile wireless communications systems. In July 1992, he transferred to NTT DoCoMo, where he researched Code-Division Multiple-Access techniques for Mobile Communication Systems. In April 1994, he transferred to NTT America, where he served as a Senior Technical Advisor of a joint project between NTT and NEXTEL Communications. In March 1996, he returned to NTT DoCoMo, where he served as a Head of the Radio Signal Processing Laboratory until August of 2001; He worked on adaptive signal processing, multiple-input multiple-output turbo signal detection, interference cancellation, and space-time coding techniques for broadband mobile communications.

In March 2002, he moved to University of Oulu, Finland, where he served as a Professor at Centre for Wireless Communications. In 2006, he served as a Visiting Professor at Ilmenau University of Technology, Ilmenau, Germany, funded by the German MERCATOR Visiting Professorship Program. Since April 2007, he has been serving as a Professor at Japan Advanced Institute of Science and Technology (JAIST), Japan, while also keeping the position at University of Oulu.

T. Matsumoto has been appointed as a Finland Distinguished Professor for a period from January 2008 to December 2012, funded by the Finnish National Technology Agency (Tekes) and Finnish Academy, under which he preserves the rights to participate in and apply to European and Finnish national projects. He is a recipient of IEEE VTS Outstanding Service Award (2001), Nokia Foundation Visiting Fellow Scholarship Award (2002), IEEE Japan Council Award for Distinguished Service to the Society (2006), IEEE Vehicular Technology Society James R. Evans Avant Garde Award (2006), and Thuringia State Research Award for Advanced Applied Science (2006), 2007 Best Paper Award of Institute of Electrical, Communication, and Information Engineers of Japan (2008), and Telecom System Technology Award by the Telecommunications Advancement Foundation (2009).